Definition of parameters for quality assurance of flattening filter free (FFF) photon beams in radiation therapy

A. Fogliata[a)]
Oncology Institute of Southern Switzerland, Medical Physics Unit, Bellinzona CH-6500, Switzerland

R. Garcia
Institut Sainte Catherine, Medical Physics Unit, Avignon F-84000, France

T. Knöös
Radiation Physics, Skåne University Hospital, Lund S-22185, Sweden and Department of Medical Radiation Physics, Lund University, Lund S-22185, Sweden

G. Nicolini, A. Clivio, and E. Vanetti
Oncology Institute of Southern Switzerland, Medical Physics Unit, Bellinzona CH-6500, Switzerland

C. Khamphan
Institut Sainte Catherine, Medical Physics Unit, Avignon F-84000, France

L. Cozzi
Oncology Institute of Southern Switzerland, Medical Physics Unit, Bellinzona CH-6500, Switzerland

(Received 6 June 2012; revised 11 September 2012; accepted for publication 11 September 2012; published 3 October 2012)

Purpose: Flattening filter free (FFF) beams generated by medical linear accelerators have recently started to be used in radiotherapy clinical practice. Such beams present fundamental differences with respect to the standard filter flattened (FF) beams, making the generally used dosimetric parameters and definitions not always viable. The present study will propose possible definitions and suggestions for some dosimetric parameters for use in quality assurance of FFF beams generated by medical linacs in radiotherapy.
Methods: The main characteristics of the photon beams have been analyzed using specific data generated by a Varian TrueBeam linac having both FFF and FF beams of 6 and 10 MV energy, respectively.
Results: Definitions for dose profile parameters are suggested starting from the renormalization of the FFF with respect to the corresponding FF beam. From this point the flatness concept has been translated into one of "unflatness" and other definitions have been proposed, maintaining a strict parallelism between FFF and FF parameter concepts.
Conclusions: Ideas for quality controls used in establishing a quality assurance program when introducing FFF beams into the clinical environment are given here, keeping them similar to those used for standard FF beams. By following the suggestions in this report, the authors foresee that the introduction of FFF beams into a clinical radiotherapy environment will be as safe and well controlled as standard beam modalities using the existing guidelines. [http://dx.doi.org/10.1118/1.4754799]

Key words: quality assurance, flattening filter free beams, dosimetric parameter definition

I. INTRODUCTION

Conventional medical linear accelerators delivering photon beams are equipped with a flattening filter (FF) in order to allow delivery of homogeneous dose distributions with broad beams. This idea was important previously, when conventional fields were used for radiotherapy in conjunction with a simple setup, e.g., parallel opposed and four field box techniques. The advance of new technologies has led to new modalities, e.g., intensity modulated therapy (IMRT) with stationary gantry angles, or rotational IMRT (VMAT, volumetric modulated arc therapy), or helical IMRT (tomotherapy). These new modalities do not need to produce a flat homogeneous beam directly. Recently, many studies focused on nonflattened beams, analyzing their characteristics and possible clinical use has been reported.[1–3] Flattening filter free (FFF) beams present unflattened, forward peaked beam, and are available as options on commercial clinically functional linear accelerators.

Physical and dosimetric differences between standard FF and unflattened FFF beams have been analyzed by various groups both through measurements and/or using Monte Carlo simulations on modified or clinically available linacs. The main issues are summarized in the paper from Georg *et al.*[4] They rely mainly on general beam characteristics,[5–14] spectrum, beam energy and depth doses,[15–18] backscatter,[19] electron contamination,[20] out of field dose,[10,11,20,21] neutron production,[20,22,23] and shielding requirements.[24,25]

Standardized and consolidated beam parameters as described or referenced in, for example, AAPM TG 142,[26] are used today for the quality assurance of flat photon beams, e.g., flatness, symmetry, and penumbrae. Those parameters are not useful directly for the new FFF beams. There is therefore the need to find new parameters for radiotherapy beams that could be usable for both standard FF and FFF beams, without creating a parallel system for the latter, and also (and most importantly), not to lose the acquired experience of standard FF beams from previous years.

In order to establish specific recommendations required by the inhomogeneous beams and high dose rates, a questionnaire concerning all the physical and dosimetric aspects that could potentially require an adjustment in current quality assurance protocols or parameter definitions was distributed among some of the first users of the currently available clinical FFF linear accelerator (i.e., Varian TrueBeam users). Their answers helped to identify some of the new quality assurance parameter definitions.

The aim of the present study is to propose possible new definitions and/or modification to existent quantities and parameters for the dosimetric issues of quality assurance for FFF beams generated by standard C-arm based medical linacs (Tomotherapy or Cyberknife units are not included in the present work). Starting from standard sets of measurements on both FFF and FF beams (even if already published and well known beams) allowed the translation of quality control metrics from FF to FFF beams. Some of those are applicable to both beam modalities, while others require new methodologies to be established in a uniform set of new metrics.

Tolerance values are beyond the scope of the present work, and will be analyzed in a forthcoming study through a deep evaluation of each parameter relative to specific beam characteristic variations.

II. QUALITY ASSURANCE OF FFF BEAMS

FFF beams delivered with "conventional" medical linear accelerators have the conical flattening filter removed and replaced by a thin foil. This foil is introduced for two reasons: (a) for safety—it will stop the electron beam reaching the patient if the target collapses, and (b) producing enough signal in the ion chamber by producing electrons. Additionally, slightly less electron contamination from the primary collimator reaches the isocenter. The FFF fields present hugely different dose profiles compared with the FF beams: a profile peaked on the central axis is typical of a medium-large sized FFF fields (Fig. 1). The widely used concepts for defining FF beam parameters would be modified in order to adapt their interpretation to FFF beams, while keeping the main concepts valid for both FFF and FF modalities.

The differences between FFF and FF in terms of quality assurance is mainly related to beam dosimetry, and not to mechanical characteristics of the linear accelerator, for which the standard quality assurance procedures still hold. It is clearly not necessary to introduce any modification to a consolidated quality assurance process for nondosimetric checks.

Data in this work are from clinically released Varian TrueBeam (Varian Medical Systems, Palo Alto, CA) facilities, having 6 and 10 MV standard FF and the new FFF beams. For this machine type, the flattening filter is replaced in FFF mode with a copper foil about 1 mm thick. This foil is the same for all energies which results in the following nominal maximum dose rates of 1400 and 2400 MU/min for 6 and 10 MV FFF, respectively (600 MU/min for standard beams). Therefore, the dose per pulse for FFF beams is up to four times higher than in standard FF beams, depending on energy.

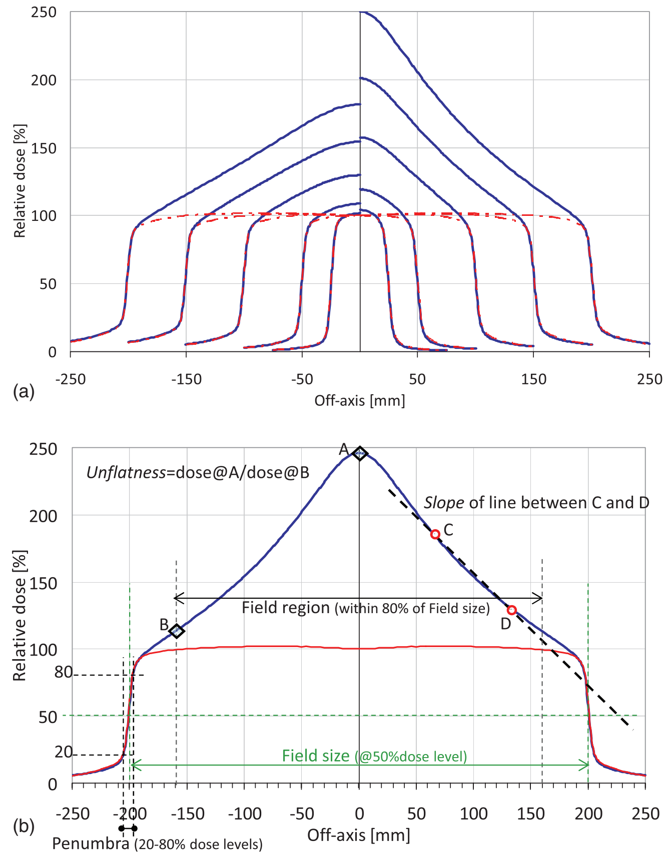

FIG. 1. (a) Profiles of 6 and 10 MV FFF (solid line) and FF (dashed line), SSD = 90 cm, $d = 10$ cm, for different field sizes. (b) Schematic description of some of the beam parameters: field region, field size, penumbra, unflatness, and slope. Point A: central axis; point B: off-axis at 80% of the field size (edge of field region); point C: off-axis at 1/3 of the field size; and point D: off-axis at 2/3 of the field size.

The concepts presented here follow the requirements which appeared in the questionnaire answers from the surveyed users. In summary the requests focused on the beam profile parameter modifications (flatness, symmetry, and penumbra), as they are no longer directly applicable to the new FFF beams. Responses on the questionnaire relating to energy spectrum, dose rate, and dose calibration suggested that we should keep the usual definitions.

II.A. Profile normalization

Based on the fact that FFF beams deliver higher dose to the central axis (as no flattening filter attenuates the beam), FFF and FF beams should be mutually renormalized to superimpose the profile fall-off (field edge).

Two methods can be followed: the inflection point or the renormalization value. Both methods hold only for symmetric beams. In the same way, all subsequent definitions will be valid only in the case of symmetric beam quality assurance.

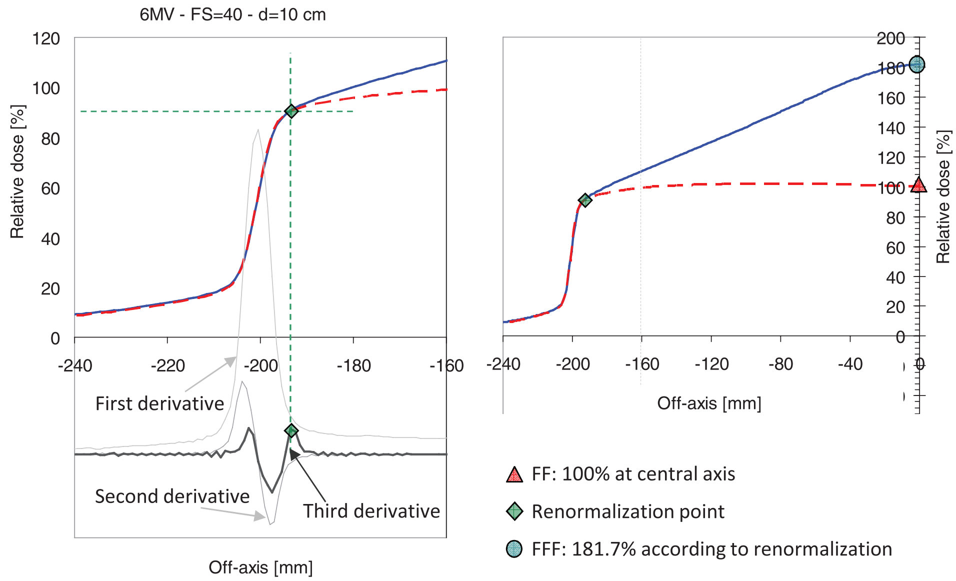

FIG. 2. Renormalization point obtained through the profile third derivative.

This is problematic for FFF beams, where the beam profile of asymmetric jaw setting fields presents strongly different dose levels toward the two beam edges, asymmetrically placed relatively to the central axis.

II.A.1. The inflection point

Pönisch *et al.*[7] suggested the use of the inflection point at the field edge to renormalize a FFF beam to the same dose level of a FF beam. From this renormalized profile it is then possible to evaluate penumbra (as the usual distance between 20% and 80% dose levels) and the field size (at the inflection point, or at 50% dose level to keep the common dosimetric field size definition).

At the inflection point, the second derivative is null (and the first derivative presents a minimum or a maximum). The easiest way to determine the position of the inflection point, not knowing the mathematical expression of the profile, is to plot the dose difference of two adjacent measuring points, ΔD. The off-axis position of the minimum or maximum at the field edge represents the inflection point. The location of this point is proximal to the 50% for standard beams normalized to the central axis, and is at the highest gradient, that could be of the order of 10%/mm. This means that the position of the inflection point can be accurately determined only with very fine measurement stepping. A common step length used for measurements in the penumbra region is one millimeter. With such a precision, together with the detector size and type in a high gradient region, the dose level that is then used for profile normalization (according to Pönisch *et al.*) could be affected easily by a 10% error. This uncertainty value is then enhanced at the beam central axis, and, for a FFF beam that has a dose level at the central axis of about 200% with respect to its corresponding FF beam, the central axis dose level could vary by up to 40% due to the normalization to the inflection point. While the measurement stepping can be finer than 1 mm to reduce possible uncertainty due to the precision, this is generally not used in common periodic quality assurance measurements nor during commissioning.

II.A.2. The renormalization value

To overcome the uncertainty using the inflection point method, another normalization point should be determined. The renormalization method is conceptually similar to the inflection point, and comes to the determination of a point in the profile shoulder of FF beam profiles to renormalize the FFF beam to the same dose level of the FF beam at that point. The "shoulder point" is located in a shallow dose gradient region, and in a region where the two FFF and FF beams present similar shapes, before the FFF beams starts to increase in dose toward the beam central axis. This point could be found as a maximum in the profile third derivative (Fig. 2).

The procedure for its determination is listed here:

- The FFF and the standard FF beam have to be mutually aligned in the off-axis direction (both centered relative to the central axis).
- Normalize the standard beam (FF) as usual, to 100% at beam central axis (triangle symbol on the right of Fig. 2).
- Compute the third derivative (as ΔD from measurements) in the penumbra region. This will present two maxima (mimima) in the ascending (respectively descending) profile edge. (The third derivative could be obtained from both FFF and FF beams, but for consistency the FF beam should be used).
- The relative dose on the FF profile corresponding to the off-axis position of the second maximum for the left profile edge—closer to the central axis—(first minimum for the right profile edge) is used to normalize the FFF beam profile at the same off-axis position (diamond symbol in Fig. 2).

TABLE I. Renormalization factors for 6 and 10 MV FFF.

Energy	Field side (cm)	$d = d_{max}$	$d = 50$ mm	$d = 100$ mm	$d = 200$ mm	$d = 300$ mm
6 MV FFF	3	101.8	101.3	100.5	100.7	99.8
	5	101.9	102.0	101.7	101.7	101.8
	10	110.1	109.8	108.7	108.7	107.6
	15	120.9	120.0	118.9	116.2	114.8
	20	133.3	132.1	129.7	125.6	122.7
	25	147.0	144.9	141.6	135.6	131.7
	30	161.6	158.8	154.2	146.8	140.1
	35	177.4	174.1	167.4	157.2	150.4
	40	194.4	189.7	181.7	169.7	158.9
10 MV FFF	3	103.3	102.6	100.5	100.3	100.8
	5	104.5	104.1	104.1	104.0	104.2
	10	120.3	120.6	119.2	118.1	117.5
	15	140.4	140.0	137.9	134.5	132.4
	20	162.1	160.7	157.6	151.9	148.1
	25	185.4	184.4	179.6	170.2	164.0
	30	210.7	208.5	201.0	188.8	181.4
	35	239.7	235.8	226.8	211.2	198.0
	40	265.8	262.1	250.1	229.8	215.0

– The relative dose at the FFF beam central axis is the renormalization value (circle symbol in Fig. 2).

The renormalization values depend on the beam as well as field size and depth. The linac construction will also influence this but as mentioned above this paper only covers the clinically available linacs.

It is assumed that beams coming from the same linear accelerator construction would give similar profile shapes, for both FFF and FF beams. Three units have been checked, and data are consistent across those different installations. With this assumption, the renormalization values from FF to FFF beams at central axis can be predetermined as a function of field size and measuring depth. These values can either be tabulated, or calculated by an analytical expression with predetermined fitting parameters. The stated values for a specific linac construction will have some tolerance intervals, leading to possible uncertainty. Determination of the renormalization values has been done in this work for 6 and 10 MV FFF beams. Data were acquired at SSD = 90 cm. In Table I, the renormalization values for 6 and 10 MV FFF are given.

Data have been fitted according to the formula:

$$\text{Renormalization} = \frac{a + b \cdot \text{FS} + c \cdot \text{depth}}{1 + d \cdot \text{FS} + e \cdot \text{depth}}, \tag{1}$$

where FS is the field side in cm, depth is the measuring depth in cm, and a, b, c, d, e are the fitting parameters. In Table II, these parameters are reported for 6 and 10 MV FFF for the studied linacs. All fits presented a root mean square $r^2 > 0.999$. In Fig. 3, the tabulated data as well as the fitting surface are plotted also to visually display the renormalization pattern as a function of field size and depth.

II.B. Dosimetric field size

Once the FFF beams are renormalized as above, the concept of dosimetric field size as the distance between the 50% dose levels can be used for FFF beams, as for FF beams [generally the full width half maximum (FWHM) is used for standard FF beams normalized to 100% at central beam axis].

Alternatively, as suggested by Pönisch *et al.*[7] the distance between the left and right inflection points could be used. But this definition suffers the uncertainty described above.

II.C. Penumbra

Penumbra can be defined according to existing protocols, e.g., by the distance between the 20% and the 80% dose levels in the field edge once the profiles are mutually renormalized as suggested above.

II.D. Unflatness, slope, peak position, and symmetry

The flatness parameter is used for standard beams to evaluate the dose variation within the central beam region (which should be kept minimal for standard FF beams). This method is not applicable for FFF beams thus the shape of the profile

TABLE II. Fit parameters for renormalization factor calculation, for 6 and 10 MV FFF.

Energy (MV)	6 FFF	10 FFF
a	95.60	89.08
b	0.6595	2.4826
c	0.1255	0.1152
d	– 0.0099	– 0.0078
e	0.0013	0.0011

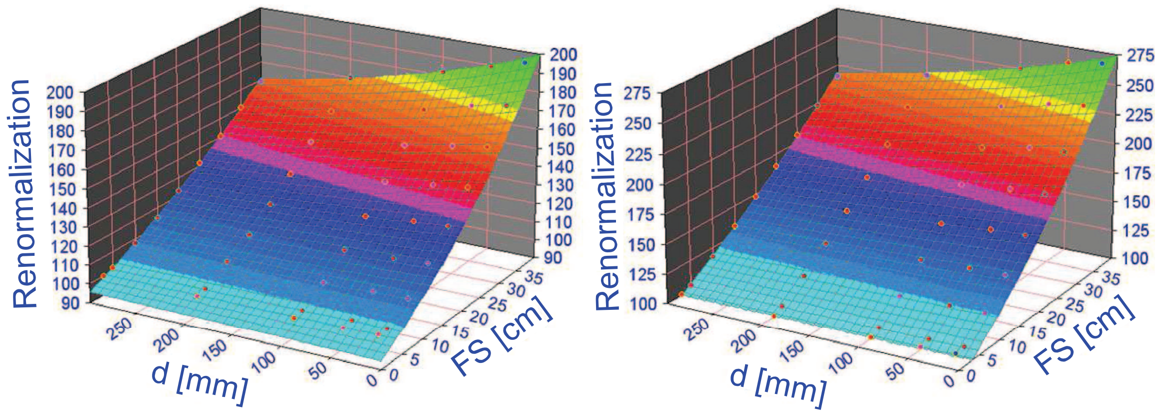

FIG. 3. Renormalization for 6 (left) and 10 (right) MV FFF, SSD = 90 cm. Surface fits the data.

has to be characterized by other parameters. It is here proposed to use the unflatness, the slope, and the peak position as defined below.

Some of the beam parameters are outlined in Fig. 1(b).

II.D.1. Flattened region and field region

The concept of flatness used in FF beams must be modified for FFF beams. The flatness is based on the flattened region definition, and should be applied to a "field region" in a way that it could be used for both beam modalities.

Once renormalized as above, the "field region" can be defined as the region within a certain defined percentage of the field (as defined by the field size), e.g., 80%. The percentage could be the same for all field sizes, or it can be changed, e.g., for field sizes <10 cm the field region is the area within the 60% of the field, and for field sizes ≥10 cm the field region is the area within the 80% of the field. In principle any definition for flattened region can be translated into a field region, according to the different protocols (e.g., Refs. 27–29).

All the following parameters should be evaluated inside the field region.

II.D.2. Flatness and unflatness

Unflatness is the parameter relative to FFF beams corresponding to flatness for FF beams. Unflatness can be defined as the ratio between the dose level at the beam central axis and the dose level at a predefined distance from the central axis as a function of field size, or at the edge of the field region [Eq. (2)]. The former method was also suggested by Georg *et al.*,[4] where the 80% of the field size was proposed. In all cases a stable definition at least of the field size has to be set before,

$$\text{Unflatness} = \frac{\text{Dose}_{\text{central.axis}}}{\text{Dose}_{\text{X.off-axis}}}, \tag{2}$$

TABLE III. Unflatness, defined as with X off-axis = 80% of field size for field side ≥10, 60% for field side <10; for 6 and 10 MV FFF.

Energy	Field side (cm)	$d = d_{max}$	$d = 50$ mm	$d = 100$ mm	$d = 200$ mm	$d = 300$ mm
	3	1.035	1.039	1.041	1.042	1.036
	5	1.023	1.031	1.033	1.034	1.032
	10	1.095	1.113	1.127	1.138	1.141
	15	1.160	1.180	1.199	1.214	1.224
6 MV FFF	20	1.243	1.259	1.279	1.303	1.311
	25	1.332	1.346	1.365	1.391	1.406
	30	1.424	1.437	1.456	1.483	1.500
	35	1.523	1.533	1.549	1.580	1.599
	40	1.626	1.634	1.650	1.681	1.713
	3	1.058	1.071	1.066	1.065	1.062
	5	1.045	1.055	1.055	1.056	1.053
	10	1.194	1.209	1.218	1.224	1.228
	15	1.325	1.338	1.348	1.36	1.368
10 MV FFF	20	1.476	1.486	1.5	1.512	1.518
	25	1.636	1.651	1.661	1.671	1.679
	30	1.8	1.819	1.826	1.836	1.845
	35	1.968	1.99	1.996	2.008	2.016
	40	2.152	2.177	2.178	2.191	2.202

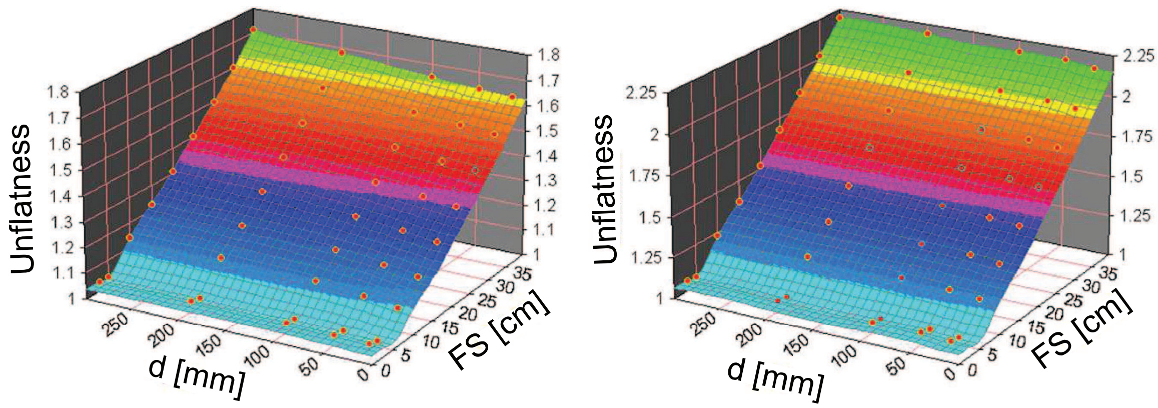

FIG. 4. Unflatness for 6 (left) and 10 (right) MV FFF.

where the numerator is the central axis dose level and the denominator is the dose level at a certain off-axis position (e.g., 80% of field size). The values could be tabulated for different conditions of field size, depth and energy to establish a sort of standard matrix for FFF unflatness.

Table III reports, for both 6 and 10 MV FFF, unflatness values for different field sizes and depths, considering X off-axis = 80% of field size for field side ≥10, 60% for field side <10, for SSD = 90 cm, and d = 10 cm profiles. In Fig. 4 the same data are plotted to visually display the unflatness parameter as a function of field size and depth.

II.D.3. Slope

The peak shape of the FFF profile can be defined by the "slope" parameter describing the left and right inclinations of the profiles. Because the FFF profile depends on the energy, with different shapes in terms of concavity or convexity of the slopes, a more general definition for a gradient of the two sides of the profile needs to be defined. This parameter can be the slope of the line passing through two fixed points on the profiles located at 1/3 and 2/3 of the half beam (defined by the field size), according to

$$\text{Slope} = \frac{(x_1 - x_2) \times (y_1 - y_2)}{(x_1 - x_2)^2}, \tag{3}$$

where x_1, y_1 are the coordinates (as dose value y at position x) on the half-profile for the first point (at −2/3 for the left, +1/3 for the right half-profile), and x_2, y_2 are the coordinates of the second point. In Fig. 1(b) the line defining the slope is reported, for better understanding, for the 10 MV FFF profile of the largest field.

The slope parameter has two aims: on one side it assures that the beam is symmetric around the collimator axis (together with the symmetry parameter) by checking its value along the main axes; on the other side its value assures the correctness of the beam energy (similarly to the beam quality parameters, even if in an indirect way). In Table IV the slope parameter for 6 and 10 MV FFF is recorded for different field sizes, for SSD = 90 cm. As argued from Table IV, slope

TABLE IV. Slope parameter for 6 and 10 MV FFF.

Energy	Field side (cm)	$d = d_{max}$	d = 50 mm	d = 100 mm	d = 200 mm	d = 300 mm
6 MV FFF	3	1.030	1.060	0.948	0.917	0.787
	5	0.338	0.414	0.414	0.370	0.333
	10	0.307	0.349	0.364	0.359	0.345
	15	0.380	0.387	0.403	0.387	0.360
	20	0.435	0.438	0.437	0.403	0.372
	25	0.484	0.473	0.457	0.421	0.383
	30	0.515	0.495	0.473	0.429	0.392
	35	0.543	0.518	0.489	0.435	0.392
	40	0.565	0.540	0.510	0.444	0.403
10 MV FFF	3	1.470	1.559	1.544	1.361	1.199
	5	0.649	0.729	0.713	0.635	0.575
	10	0.645	0.648	0.631	0.588	0.544
	15	0.748	0.742	0.715	0.654	0.597
	20	0.819	0.801	0.759	0.684	0.616
	25	0.856	0.837	0.779	0.700	0.622
	30	0.884	0.864	0.800	0.704	0.627
	35	0.900	0.879	0.823	0.707	0.626
	40	0.909	0.883	0.812	0.703	0.614

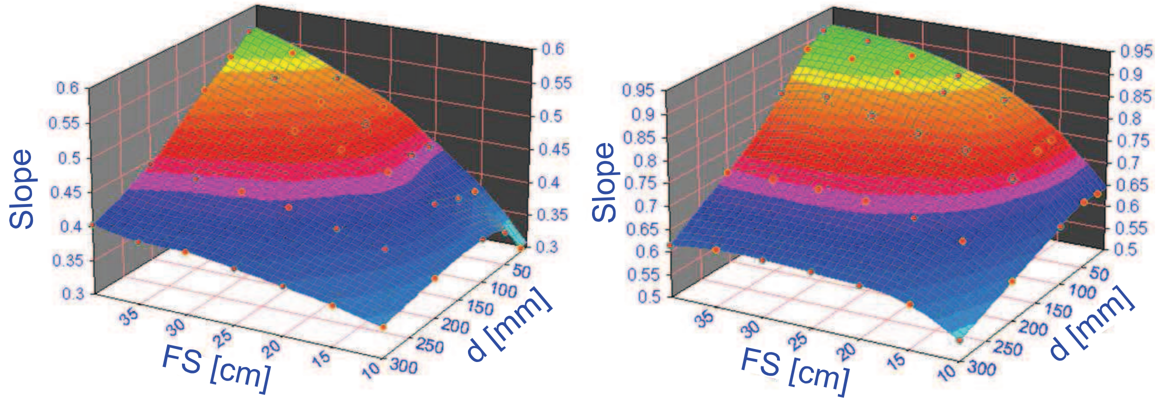

FIG. 5. Slope for 6 (left) and 10 (right) MV FFF, from field ≥10 cm side.

values for field sizes smaller than 10 cm are rather inconsistent, as the small fields lies in the broad profile peak that is rather homogeneous. In particular, for fields of 3 cm side the slope is larger than 1 (more for 10 MV FFF), and the two points for calculating the slope are on the profile shoulder, leading to a meaningless value. The slope parameter should hence be evaluated only for fields equal or larger than 10 cm side. In Fig. 5 the same data are plotted to visually display the slope parameter as a function of field size and depth.

II.D.4. Peak position

The peak of the FFF profile is the indication of the forward direction of the beam. Intuitively this peak should be located on the beam central axis. In ideal conditions the two slopes should be equal in absolute value and they should intersect on the beam central axis. The "peak position" parameter is defined as the off-axis position of the intersection point of the left and right slopes, as follows:

$$\text{Peak position} = \frac{(I_L - I_R)}{(S_R - S_L)}, \tag{4}$$

where I_L and I_R are the left and right intercepts, respectively; S_L and S_R are the left and right slopes, respectively. The intercepts are calculated as

$$I = y_2 - x_2 \times \frac{(x_1 - x_2) \times (y_1 - y_2)}{(x_1 - x_2)^2} \tag{5}$$

with x_1, y_1 and x_2, y_2 as in the slope parameter definition.

II.D.5. Symmetry

Symmetry, as a parameter checking the equality level between left and right sides of a profile, can be defined as usual for standard FF beams, with the only difference that the evaluation area should be within the field region for FFF beams instead of the flattened region commonly used in FF beams. Examples of common measures of symmetry are given in Eq. (6).

$$-\text{The maximum dose ratio}: \left(\frac{D_x}{D_{-x}}\right)_{\max}, \tag{6a}$$

where D_x and D_{-x} are the doses at x and $-x$ positions (symmetric relative to central axis).

$$-\text{The area ratio}: \left|\frac{\text{LeftIntegral} - \text{RightIntegral}}{\text{LeftIntegral} + \text{RightIntegral}}\right| \cdot 2, \tag{6b}$$

where LeftIntegral (and RightIntegral) are the areas bounded by the profile on the left (and right) of the beam central axis,

$$-\text{The maximum variation}: (D_x - D_{-x})_{\max}, \tag{6c}$$

where D_x and D_{-x} are the doses at x and $-x$ positions (symmetric relative to central axis).

II.E. Energy spectrum and quality index

FFF beams present an energy spectrum significantly different from FF beams since the thick conical shaped attenuator is removed. This results generally in a softer beam (especially for the included linac construction) with less scattered electrons. The energy spectrum is also almost invariant across the field compared to a flattened beam where the energy decreases from central axis toward edges.

The energy spectrum is an entity not directly measurable in a radiotherapy department, and quality index methods to achieve dosimetric parameters based on depth dose curves are commonly used. Despite the differences in the FFF spectrum with respect to the corresponding FF beam, there is no reason to change quality index definitions that can be, for example:

- TPR ratio: $TPR_{10}^{20} = \frac{TPR(20\text{ cm})}{TPR(10\text{ cm})}$ for a 10×10 cm^2 field. This parameter can be easily measured or obtained from depth dose curves[30] as quality index: QI $= 1.2661 \cdot D_{20\text{cm}} / D_{10\text{ cm}} - 0.0595$.
- Depth of maximum dose, $d_{\max}$, and percentage depth dose at 10 cm, %dd(10), for a 10×10 cm^2 field, SSD $= 100$ cm.
- Depth dose ratio between 20 and 10 cm depths, often called ionization ratio: J $= \frac{D_{20\text{ cm}}}{D_{10\text{ cm}}}$ for a 10×10 cm^2 field, SSD $= 100$ cm.

Examples of quality indices for 6 and 10 MV FFF and FF beams are reported in Table V.

TABLE V. Beam quality indices for 6 and 10 MV beams from a TrueBeam. Values are averaged from three TrueBeam facility (error refers to 1 SD).

Energy (MV)	TPR_{10}^{20}	QI	%dd (10 cm)	$J = D_{20}/D_{10}$
6 FFF	0.631 ± 0.005	0.632 ± 0.004	63.6 ± 0.7	0.546 ± 0.003
6 FF	0.667 ± 0.004	0.668 ± 0.004	66.6 ± 0.7	0.574 ± 0.003
10 FFF	0.706 ± 0.007	0.705 ± 0.004	71.4 ± 1.0	0.604 ± 0.003
10 FF	0.740 ± 0.004	0.740 ± 0.004	73.2 ± 0.7	0.631 ± 0.003

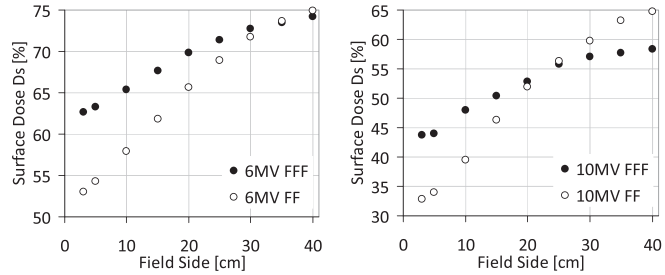

FIG. 6. Surface dose D_s at a depth of 0.5 mm, in % of the dose at d_{max}, for 6 and 10 MV, FFF and FF, SSD = 90 cm.

II.F. Surface dose

Due to different electron contamination and lower photon energy spectrum, surface doses of FFF are expected to be different from FF beams.[18] The surface dose parameter D_s is defined here as the relative dose at $d = 0.5$ mm with respect to the dose at d_{max}. In Fig. 6 surface dose for fields from 3 to 40 cm side, FFF and FF, is summarized.

II.G. Output factors

The head scatter component of a FFF beam relative to the corresponding FF beam is markedly different. This is due to the absence of the flattening filter, which is the dominating source for head scatter. Variation in output factors (defined as the ratio between the dose of a test field and the dose of a reference field in fixed standard conditions) is then less pronounced for FFF beams due to the head scatter component.

Output factor definitions are kept identical for both FFF and FF beams. Particular care has to be used in measuring and evaluating small fields, as for those sizes the source occlusion effect is present, increasing the variation of head scatter component. Proper detectors and all precautions of small field dosimetry have to be carefully considered, for both FFF and FF beams, as widely recommended. This point is of particular interest for FFF beams since a common usage is for small lesions treated stereotactical due to their high dose rate and peaked profile characteristics. An example of FFF and FF beam output factors from 2 to 40 cm field side are shown in Fig. 7, where the collimator exchange effect is also shown, for measurements in isocentric conditions, $d = 10$ cm, presenting to be less pronounced for FFF beams. To better appreciate the difference in head scatter component, Fig. 8 reports the same output factors, but measured in air, with a brass buildup cap of an equivalent thickness of 2 cm of water on the ion chamber. In both setup conditions the output factors of FFF fields are less spread, in particular for in air evaluation, confirming the lower head scatter component for such fields.

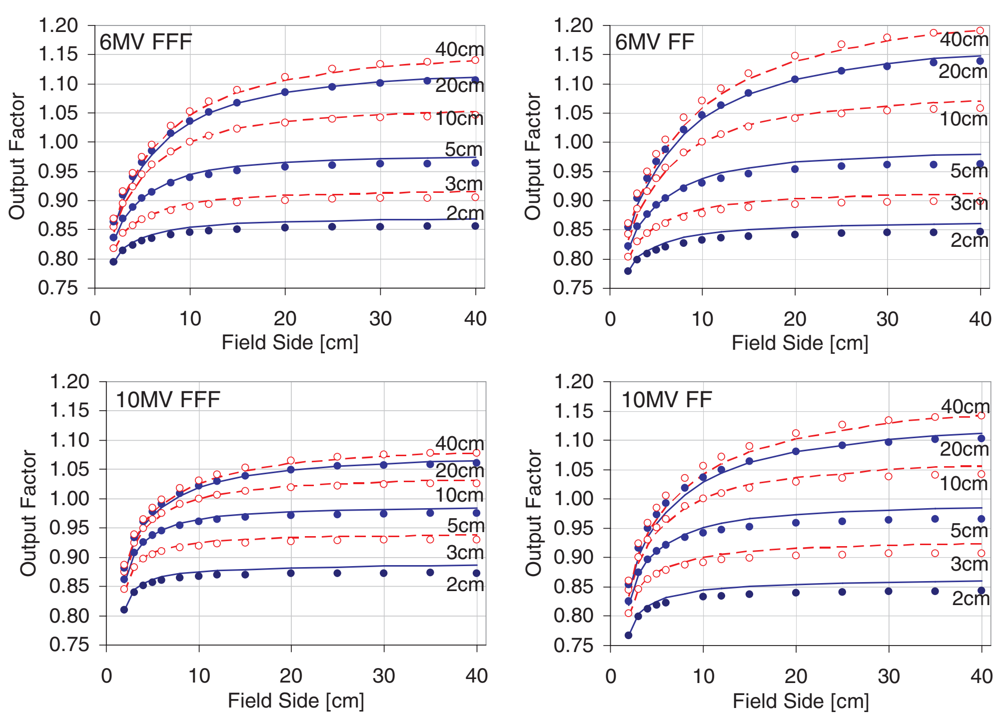

FIG. 7. Output factors in water at isocentre, $d = 10$ cm, for 6 and 10 MV, FFF and FF. Lines refer to fixed X jaws and symbols to fixed Y jaws.

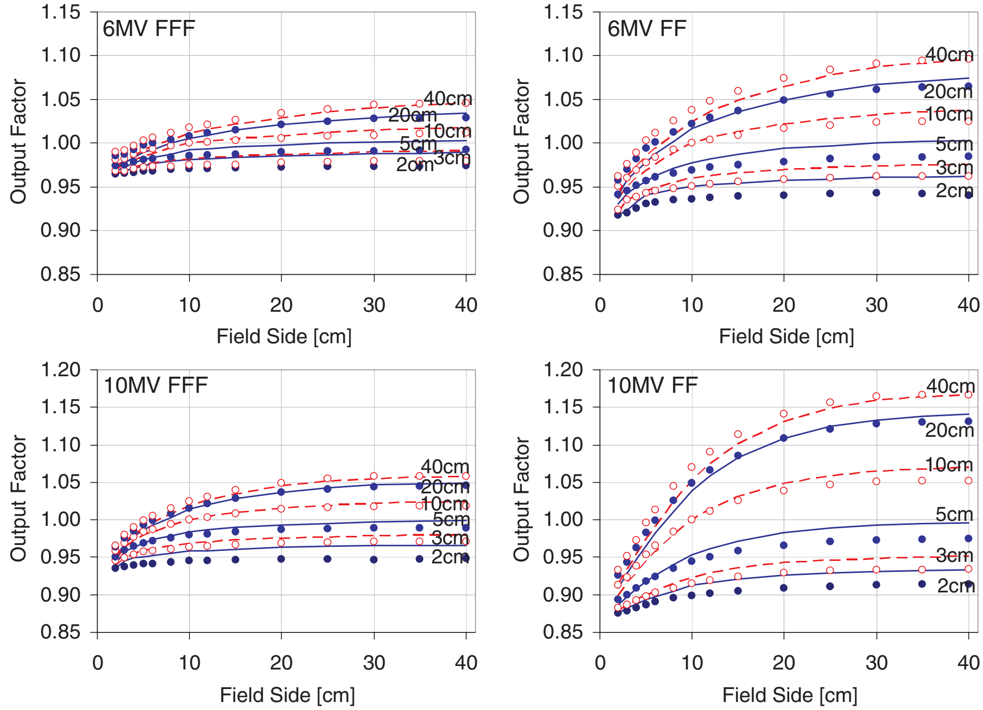

FIG. 8. Output factors in air at isocentre, for 6 and 10 MV, FFF and FF. Lines refer to fixed X jaws and symbols to fixed Y jaws.

II.H. Dose rate

Characteristic of the FFF beams is the increase in dose rate (and dose per pulse in TrueBeam facilities). This is two to four times higher than standard beams. The common check on dose rate dependence has to be performed on the entire dose rate range, keeping the consolidated experience in use for FF beams. For FFF beams particular attention has to be paid in the dosimetry system choice: the collection efficiency of ionization chambers, the possible saturation are just examples to consider for correct measurements.

II.I. Absolute dose calibration

Absolute calibration of the beam output shall follow dedicated protocols (e.g., Refs. 30 and 31). There is no reason to change the reference conditions for calibration, but there is a need for a re-evaluation of the beam quality factor (k_Q) values for FFF beams in relation to beam quality indices, as they are not listed as clinical used beams. k_Q data from the detectors used in the present work are listed in the first part of Table VI. Several studies have shown that the conventional methods of quality index give slightly erroneous data for stopping power ratios;[15,17] however, the codes of practice[30,31] are still important to maintain traceability by following these indices until new recommendations are available.

To note is that the recombination factor k_s changes slightly between FFF and FF beams, but this difference is systematic. Measured factors on TrueBeam beams (presenting high dose per pulse in FFF mode) from different centers, using different protocols, procedures, and dosimetric systems to evaluate k_s are reported in the second part of Table VI. For the included

TABLE VI. Quality factors k_Q and ion recombination factors k_s for 6 and 10 MV beams for different ion chambers. Chamber volume and operating applied voltage are detailed in the last column.

Detector	6 FFF	6 FF	10 FFF	10 FF	Volume, tension
			k_Q (TPR_{10}^{20})		
PTW 30013	0.994 (0.630)	0.990 (0.664)	0.983 (0.705)	0.975 (0.737)	0.6 cm^3, +400 V
PTW 30013	0.997 (0.623)	0.993 (0.660)		0.981 (0.734)	0.6 cm^3, +400 V
NE 2571	0.997 (0.636)	0.994 (0.671)	0.990 (0.713)	0.985 (0.743)	0.6 cm^3, −250 V
			k_s		
PTW 30013	1.005	1.003	1.008	1.003	0.6 cm^3, +400 V
PTW 30013	1.006	1.002		1.003	0.6 cm^3, +400 V
NE 2571	1.012	1.005	1.024	1.006	0.6 cm^3, −250 V
CC04, Scanditronix	1.007	1.004	1.012		1 cm^3, +300 V
CC25, Scanditronix	1.010	1.005	1.018		0.25 cm^3, +300 V
Exradin A16	1.001	1.000	1.002		0.007 cm^3, +400 V

facilities the dose per pulse is the same for all dose rate settings, thus also the recombination factor is the same.

III. CONCLUSIONS

We have presented ideas regarding the quality controls (QC) that have to be considered during the establishment of a quality assurance program (QA) when introducing FFF beams into a clinical setting. These ideas have been discussed and we have tried to keep them in accordance with and similar to those used for standard FF beams. In this paper we have also setup some expectation values for some of the proposed parameters. By following the recommendations in this report we foresee that the introduction of FFF beams into the clinic will be as safe for the patient as other radiotherapy procedures existing in the radiation oncology community today.

ACKNOWLEDGMENTS

The authors are very grateful to Yanai Krutman from Rabin Medical Center—Beilinson Hospital, Davidoff Cancer Center—Radiotherpay Physics—Petah Tikvah Israel, for providing some data on recombination factors. Thanks also to Lee Ambolt from the Radiation Physics of the Lund University (Sweden) for having revised the language of the paper. Luca Cozzi acts as a Scientific Advisor to Varian Medical Systems and is Head of Research and Technological Development at the Oncology Institute of Southern Switzerland, Bellinzona, Switzerland.

[a)]Authors to whom correspondence should be addressed. Electronic addresses: afc@iosi.ch and antonella.fogliata-cozzi@eoc.ch; Telephone: +41 91 8119184.

[1]S. W. Stevens, K. E. Rosser, and J. L. Bedford, "A 4 MV flattening filter-free beam: Commissioning and application to conformal therapy and volumetric modulated arc therapy," Phys. Med. Biol. **56**, 3809–3824 (2011).
[2]O. N. Vassiliev, S. F. Kry, J. Y. Chang, P. A. Balter, U. Titt, and R. Mohan, "Stereotactic radiotherapy for lung cancer using a flattening filter free Clinac," J. Appl. Clin. Med. Phys. **10**, 14–21 (2009).
[3]M. Scorsetti *et al.*, "Feasibility and early clinical assessment of flattening filter free (FFF) based stereotactic body radiotherapy (SBRT) treatments," Radiat Oncol. **6**, 113 (2011).
[4]D. Georg, T. Knöös, and B. McClean, "Current status and future perspective of flattening filter free photon beams," Med. Phys. **38**, 1280–1293 (2011).
[5]J. Cashmore, "The characterization of unflattened photon beams from a 6 MV linear accelerator," Phys. Med. Biol. **53**, 1933–1946 (2008).
[6]G. Kragl, S. af Wetterstedt, B. Knäusl, M. Lind, P. McCavana, T. Knöös, B. McClean, and D. Georg, "Dosimetric characteristics of 6 and 10 MV unflattened photon beams," Radiother. Oncol. **93**, 141–146 (2009).
[7]F. Pönisch, U. Titt, O. N. Vassiliev, S. F. Kry, and R. Mohan, "Properties of unflattened photon beams shaped by a multileaf collimator," Med. Phys. **33**, 1738–1746 (2006).
[8]J. Hrbacek, S. Lang, and S. Klöck, "Commissioning of photon beams of a flattening filter-free linear accelerator and the accuracy of beam modeling using an anisotropic analytical algorithm," Int. J. Radiat. Oncol. Biol., Phys. **80**, 1228–1237 (2011).
[9]D. Georg, G. Kragl, S. af Wetterstedt, P. McCavana, and B. McClean, "Photon beam quality variations of a flattening filter free linear accelerator," Med. Phys. **37**, 49–53 (2010).
[10]O. N. Vassiliev, U. Titt, F. Pönisch, S. F. Kry, R. Mohan, and M. T. Gillin, "Dosimetric properties of photon beams from a flattening filter free clinical accelerator," Phys. Med. Biol. **51**, 1907–1917 (2006).
[11]O. N. Vassiliev,U. Titt, S. F. Kry, F. Pönisch, M. T. Gillin, and R. Mohan, "Monte Carlo study of photon fields from a flattening filter-free clinical accelerator," Med. Phys. **33**, 820–827 (2006).
[12]U. Titt, O. N. Vassiliev, F. Pönisch, L. Dong, H. Liu, and R. Mohan, "A flattening filter free photon treatment concept evaluation with Monte Carlo," Med. Phys. **33**, 1595–1602 (2006).
[13]A. Mesbahi, P. Mehnati, A. Keshtkar, and A. Farajollahi, "Dosimetric properties of a flattening filter-free 6-MV photon beam: A Monte Carlo study," Radiat. Med. **25**, 315–324 (2007).
[14]M. Dalaryd, G. Kragl, C. Ceberg, D. Georg, B. McClean, S. af Wetterstedt, E. Wieslander, and T. Knöös, "A Monte Carlo study of a flattening filter-free linear accelerator verified with measurements," Phys. Med. Biol. **55**, 7333–7343 (2010).
[15]G. Xiong and D. W. O. Rogers, "Relationship between%dd(10)x and stopping-power ratios for flattening filter free accelerators: A Monte Carlo study," Med. Phys. **35**, 2104–2109 (2008).
[16]O. A. Sauer, "Determination of the quality index (Q) for photon beams at arbitrary field sizes," Med. Phys. **36**, 4168–4172 (2009).
[17]C. Ceberg, S. Johnsson, M. Lind, and T. Knöös, "Prediction of stopping-power ratios in flattening-filter free beams," Med. Phys. **37**, 1164–1168 (2010).
[18]Y. Wang, M. K. Khan, J. Y. Ting, and S. B. Easterling, "Surface dose investigation of the flattening filter-free photon beams," Int. J. Radiat. Oncol. Biol., Phys. **83**, e281–e285 (2012).
[19]U. Titt, O. N. Vassiliev, F. Pönisch, S. F. Kry, and R. Mohan, "Monte Carlo study of backscatter in a flattening filter free clinical accelerator," Med. Phys. **33**, 3270–3273 (2006).
[20]A. Mesbahi, "A Monte Carlo study on neutron and electron contamination of an unflattened 18-MV photon beam," Appl. Radiat. Isot. **67**, 55–60 (2009).
[21]A. Mesbahi and F. S. Nejad, "Monte Carlo study on a flattening filter-free 18-MV photon beam of a medical linear accelerator," Radiat. Med. **26**, 331–336 (2008).
[22]S. F. Kry, R. M. Howell, U. Titt, M. Salehpour, R. Mohan, and O. N. Vassiliev, "Energy spectra, sources, and shielding considerations for neutrons generated by a flattening filter-free Clinac," Med. Phys. **35**, 1906–1911 (2008).
[23]S. F. Kry, U. Titt, F. Pönisch, O. N. Vassiliev, M. Salehpour, M. Gillin, and R. Mohan, "Reduced neutron production through use of a flattening-filter-free accelerator," Int. J. Radiat. Oncol. Biol., Phys. **68**, 1260–1264 (2007).
[24]S. F. Kry, R. M. Howell, J. Polf, R. Mohan, and O. N. Vassiliev, "Treatment vault shielding for a flattening filter-free medical linear accelerator," Phys. Med. Biol. **54**, 1265–1273 (2009).
[25]O. N. Vassiliev, U. Titt, S. F. Kry, R. Mohan, and M. T. Gillin, "Radiation safety survey on a flattening filter-free medical accelerator," Radiat. Prot. Dosim. **124**, 187–190 (2007).
[26]E. E. Klein, J. Hanley, J. Bayouth, F. F. Yin, W. Simon, S. Dresser, C. Serago, F. Aguirre, L. Ma, B. Arjomandy, and C. Liu, "Task Group 142 report: Quality assurance of medical accelerators," Med. Phys. **36**, 4197–4212 (2009).
[27]R. Nath, P. J. Biggs, F. J. Bova, C. C. Ling, J. A. Purdy, J. van de Gejin, and M. S. Weinhous, "AAPM code of practice for radiotherapy accelerators: Report of AAPM Radiation Therapy Task Group No. 45," Med. Phys. **21**, 1093–1121 (1994).
[28]IEC, "Medical electron accelerators—Functional performance characteristics," International Electrotechnical Commission Publication 976, 1989.
[29]IEC, "Medical electron accelerators in the range 1 MeV–50 MeV—Guidelines for functional performance characteristics," International Electrotechnical Commission Publication 977, 1989.
[30]IAEA, "Absorbed dose determination in external beam radiotherapy," Technical Reports Series No. 398 (International Atomic Energy Agency, Vienna, 2000).
[31]P. R. Almond, P. J. Biggs, B. M. Coursey, W. F. Hanson, M. S. Hug, R. Nath, and D. W. Rogers, "AAPM's TG-51 protocol for clinical reference dosimetry of high-energy photon and electron beams," Med. Phys. **26**, 1847–1870 (1999).